ELSEVIER

Nuclear Instruments and Methods in Physics Research A 426 (1999) 229–237

NUCLEAR INSTRUMENTS & METHODS IN PHYSICS RESEARCH Section A

Use of the $K_L \to 3\pi^0$ decay as a tagged photon source to measure material thickness in a neutral kaon beam

E.D. Zimmerman*

Enrico Fermi Institute, The University of Chicago, 5640 South Ellis Avenue, Chicago, IL 60637, USA

Received 9 September 1998

Abstract

A new method for measuring the thickness (in radiation lengths) of thin windows or gas-filled regions in a high-energy neutral kaon beam is presented. Using an electromagnetic calorimeter to reconstruct the six-photon signature of a $K_L \to 3\pi^0$ decay, we search for the presence of charged tracks to measure the probability of photon conversions in material upstream of the spectrometer. A magnetic field is used in the vacuum between the decay region and the material to be measured, allowing external photon conversions to be distinguished from decay processes with an internal photon conversion such as $\pi^0 \to e^+e^-\gamma$. © 1999 Elsevier Science B.V. All rights reserved.

Keywords: Kaon beam; Mylar–Kevlar vacuum; Dalitz pairs; Clusters; Drift chambers

1. Introduction

This paper presents a technique for measuring the thickness (in radiation lengths) of thin windows in a high-energy neutral hadron beam. This technique measures directly the probability of a photon conversion in the material.

Material in a fixed-target spectrometer can be a significant source of backgrounds to rare physics processes. In experiment FNAL-E799-II, a rare K_L decay search at Fermilab, a Mylar–Kevlar vacuum window separates a vacuum decay region from the detector. Photon conversions in this window create background to rare decays with electron signatures, and bremsstrahlung in the window presents background to decay modes with both electrons and photons. Finally, multiple scattering in the vacuum window and spectrometer degrades vertex position and track momentum resolution. An accurate determination of the amount of material in the detector is necessary to simulate and correct for these effects.

In E799-I, a previous generation of this experiment, the amount of material in the detector was measured by examining electrons which passed through the detector material, and searching for photons from bremsstrahlung in the detector [1]. That technique, however, cannot distinguish between the vacuum window assembly and material farther downstream. In E799-II, the vacuum window region has instead been measured by examining conversions of photons from $K_L \to 3\pi^0 \to 6\gamma$

* Present address: Columbia University, Neris Laboratories, P.O. Box 137, Irvington, NY 10533, USA. E-mail: edz@fnal.gov.

0168-9002/99/$ – see front matter
PII: S0168-9002(98)01424-7

decays using data taken with a special detector configuration.

2. Detector overview

The E799/E832 spectrometer (Fig. 1) surrounds two nearly-parallel neutral hadron beams produced by 800 GeV protons striking a BeO target. Downstream of the target, the hadron beams were defined by collimators with a solid angle of 0.35 μstr each, aimed away from the primary beam at a targeting angle of 4.8 mrad. Photons and charged particles in the beam were removed by a lead absorber and a series of sweeping magnets. Ninety four meters from the target, the beams entered a decay region 64 m long. A vacuum window 158 m from the target defined the downstream end of the decay region. In the 0.5 m space immediately downstream of the vacuum window were several Mylar windows defining different gas volumes. These were followed immediately by the first of four drift chambers. The chambers were used to measure charged track positions in vertical and horizontal views transverse to the beams; each view consisted of two wire planes, offset by a half-cell which was 0.635 cm wide. Hit-pair position resolutions were between 90 and 110 μm. The analysis magnet shown in the figure was not used for this measurement.

Downstream of the fourth drift chamber, a set of trigger hodoscopes provided timing information for charged particles. Throughout the spectrometer, a series of nine ring-shaped photon veto counters defined the perimeter of the fiducial region transverse to the beam direction. A 3100-channel pure CsI calorimeter downstream of the trigger hodoscopes provided all photon and electron energy measurements for this study. The CsI crystals were 27 radiation lengths deep [2]. This calorimeter provided electron and photon energy resolution of better than 2% for energies above 2 GeV. The crystals in the central region of the array were 2.5 cm square in the direction transverse to the beam; in the outer region the crystals were 5 cm square. The calorimeter had two beam holes to allow the neutral beams to pass through. The inner edge of the fiducial region was defined by two more veto counters, one surrounding each beam hole. Downstream of the CsI calorimeter was a 10 cm thick lead wall and an additional scintillator plane (the "hadron veto") which was used in the trigger to reject events with hadrons.

3. Measurement technique

The integrated radiation thickness from the vacuum window to the center of the first drift chamber

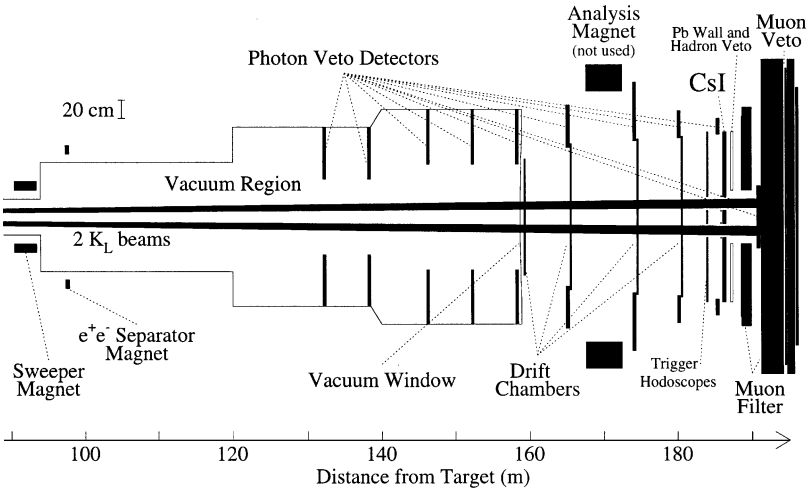

Fig. 1. The E799/E832 spectrometer configured for material thickness measurements.

was inferred from the rate of $K_L \to 3\pi^0 \to 6\gamma$ decays where one photon converted in the material.

This material (Fig. 2) included the Mylar–Kevlar vacuum window, four additional 0.001" Mylar windows, half of a drift chamber, an air gap, and two enclosed gas volumes labeled "Bag 1a" and "Bag 1b."

In order to make the acceptances similar for decays with a photon conversion and decays with no conversion (all-neutral $K_L \to 3\pi^0$ decays), a special run was taken with the spectrometer magnet off. This takes advantage of the narrow opening angle of conversion pairs and the similar response of the CsI calorimeter to electrons and photons. In the energy range above 2 GeV, nearly all conversion pairs [3] have one of two topologies: either the two electrons strike the CsI less than 4 cm apart (and form a single cluster), or the particles have such asymmetric energies that one electron is far below clustering threshold and can be lost without affecting the event kinematics significantly. Therefore, when using only the calorimeter in the reconstruction, a $3\pi^0$ analysis will find $K_L \to 3\pi^0$ events with six photons as well as those where a photon converted somewhere in the detector and the two converted electrons merged to form a sixth cluster. The large branching ratio and many kinematic constraints on this fully-reconstructed decay make non-$3\pi^0$ backgrounds negligible.

One disadvantage of this configuration was that it was not possible to calibrate the CsI using data from this special run. In normal runs, the calorimeter was calibrated using measured momenta of electrons from $K_L \to \pi e \nu$ decays. In the special run, charged track momenta could not be measured because the spectrometer magnet was off. Calibration constants obtained from nearby runs were used for the special run data, but energy resolution was not optimal when using these constants.

Once the six-cluster final state is reconstructed and gives the kaon mass, the chambers can be examined to see whether or not one of the photons converted. It would be possible to infer the photon positions and directions from the kaon recontruction using only the calorimeter, and one could search for chamber hits on the wires along the reconstructed photon paths. Many hits would indicate a photon conversion. In practice, this does not appear to work well because of accidental chamber hits and multiple-scattering of conversion electrons. Therefore, a loose tracking algorithm was used. In most conversion events, the electrons were too close together to resolve in Chamber 1, so only one of the two tracks was reconstructed (see Fig. 3).

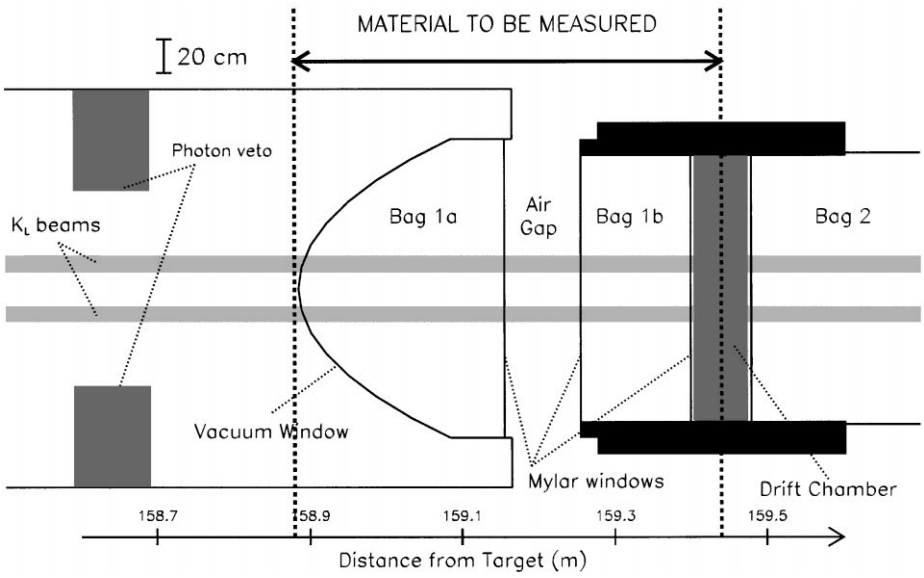

Fig. 2. Expanded view of the region of the spectrometer near the vacuum window. Note the compressed vertical scale.

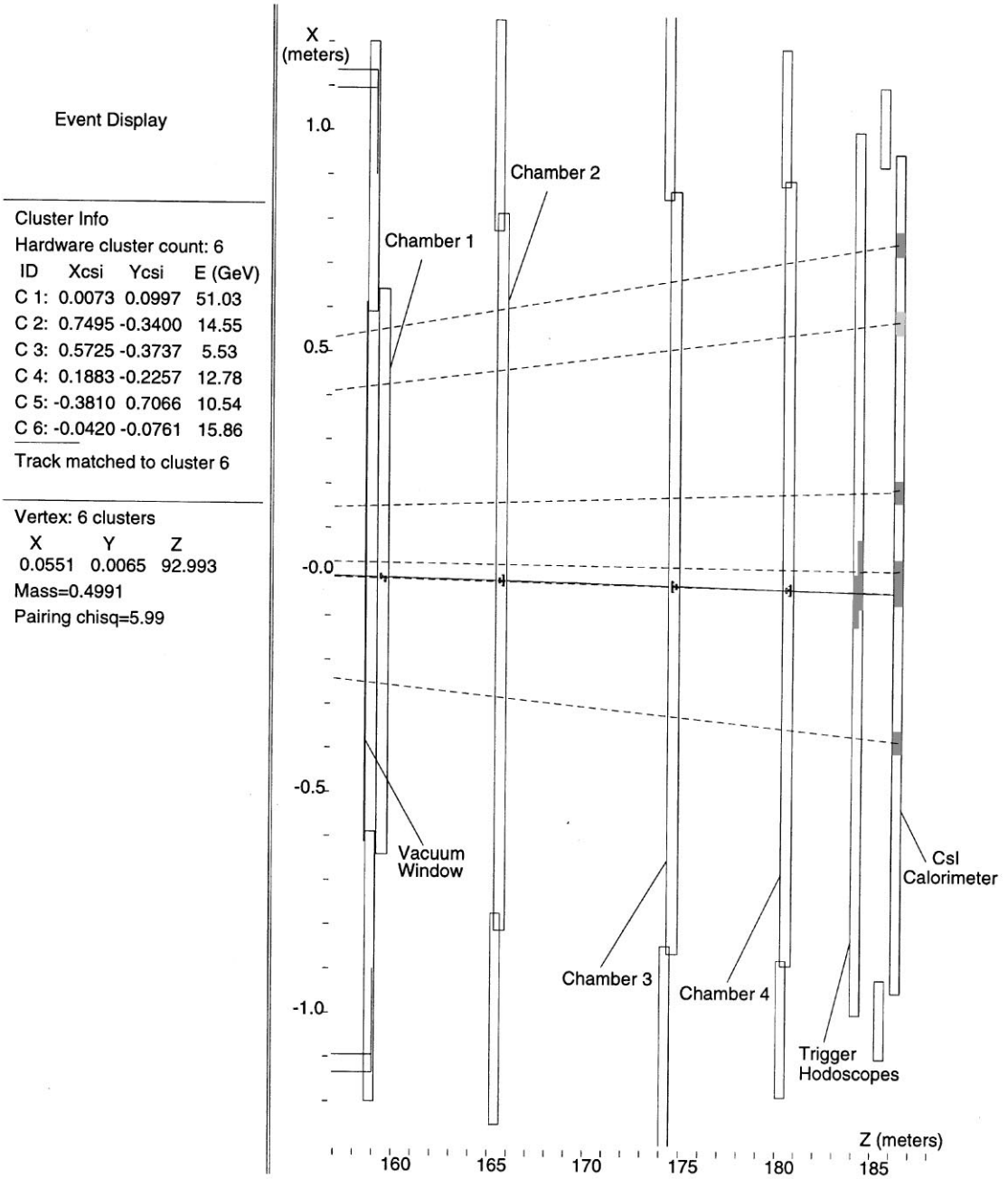

Fig. 3. Display of a candidate photon conversion at the vacuum window. The display shows a plan view of the charged spectrometer including the four drift chambers, trigger hodoscopes, and calorimeter. In-time hits are shown in all detector elements. The downstream direction is to the right. Dashed lines indicate photon directions reconstructed assuming $3\pi^0 \rightarrow 6\gamma$; the solid line indicates a reconstructed charged track. Chamber wires with in-time hits are shown as small vertical lines in the two overlapping views of each chamber. The invariant mass of the three reconstructed π^0's is equal (within resolution) to the K_L mass.

Photons which converted downstream of the center of the first chamber did not produce reconstructible tracks, so material downstream of this point was not included in the radiation thickness measurement.

There is a potentially large background to conversions from the π^0 Dalitz decay ($\pi^0 \to e^+e^-\gamma$). This mode has a branching ratio of 1.2%, and strongly favors small e^+e^- invariant mass (and therefore small opening angle). When the electrons are too close together to reconstruct a vertex, this decay is not easily distinguishable from a window conversion. With three π^0 decays in each event, the probability of one Dalitz decay is 3.5%, which is significantly higher than the probability of a photon conversion in the thin window. Although requiring the K_L decay to occur far upstream gives a longer flight distance for Dalitz electrons to separate, the background remains significant and difficult to model; Monte Carlo (MC) studies of this background show it to be critically dependent on the simulation of multiple scattering in the detector and energy deposition in the CsI.

To reduce the Dalitz background, a special separator magnet [4] was used in the decay region. This low-field dipole provided a transverse momentum kick of 10 MeV/c, which separated most Dalitz pairs enough to where they formed two separate tracks in the chambers and two clusters in the calorimeter. The center of the magnet was 97.6 m downstream of the target. The magnet components were outside the vacuum pipe, so the field covered the entire cross-section of the vacuum and did not form an additional aperture. Only kaon decays which reconstructed upstream of the separator magnet were used in the analysis. All material being measured was well downstream of this magnet.

4. Analysis

4.1. Triggers

Two triggers were used for the measurement. The first (the "charged trigger") was used to select photon conversion candidates. At least 24 GeV of in-time energy was required in the calorimeter, and a hardware cluster processor [5] required at least six clusters of connected CsI crystals with at least 1 GeV of energy per crystal. Due to the typical transverse energy profile of electromagnetic showers, this effectively applied a 2 GeV threshold on individual photon energies. In addition, this trigger required at least one hit in the vertical view of the second, third, and fourth drift chambers. Events were vetoed if more than 0.5 GeV of energy was deposited in any of the photon vetoes, or if energy consistent with a pion shower was detected in the hadron veto. The charged trigger was not prescaled.

The second trigger (the "neutral trigger") was used to record $K_L \to 3\pi^0 \to 6\gamma$ decays without a photon conversion. This trigger was identical to the charged trigger, except that it did not impose any drift chamber activity requirements. The neutral trigger was prescaled by a factor of 20.

4.2. Calorimeter analysis

The $K_L \to 3\pi^0 \to 6\gamma$ decay was reconstructed using its six photon signature in the CsI calorimeter. The calorimeter analysis was the same for both trigger types.

Events were required to have exactly six clusters of energy, with a minimum cluster energy of 2 GeV. The six clusters were arranged into pairs, and a "vertex" distance z_{12} from the calorimeter was calculated for each pair using the π^0 mass as a constraint:

$$z_{12} = \frac{\sqrt{E_1 E_2 r_{12}}}{m_{\pi^0}},$$

where E_1 and E_2 are the cluster energies and r_{12} is the distance between the clusters in the calorimeter. Of the 15 possible pairing combinations, we selected the one with the best χ^2 for the hypothesis that the three pairs came from π^0 decays at the same distance from the target along the neutral beam axis. This χ^2 was required to be less than 25 (with two degrees of freedom). The requirement was loose because cluster position and energy resolution was degraded if the photon converted far upstream, and this component of the resolution was not taken into account when calculating the χ^2. In

addition, the reconstructed $3\pi^0$ invariant mass was required to be within $20\,\mathrm{MeV}/c^2$ of the K^0 mass (Fig. 4), and the center of energy at the calorimeter was required to be within the beams. This last cut removed kaons which scattered in the absorber or collimators.

Only events with a reconstructed decay position between 91 and 97 m from the target were accepted. This short range, in the far upstream end of the vacuum decay region, accepted only decays upstream of the e^+e^- separator magnet.

MC studies show that the efficiency of the $K_L \to 3\pi^0$ reconstruction for events with a photon conversion at the vacuum window was 0.94 of the efficiency for events without one. The acceptance loss for window conversions was caused by events with a seventh cluster above 2 GeV or a bad pairing χ^2.

After the calorimeter analysis, 17 559 events remained in the data sample taken from the neutral trigger. Correcting for the prescale, acceptance, and the $\pi^0 \to \gamma\gamma$ branching ratio of 0.988, this yields a total sample of $1.44 \times 10^7 K_L \to 3\pi^0$ decays (or 6.8×10^7 total K_L decays) in the region of interest.

In the charged trigger, 17 228 events remain at this stage of the analysis. Most of these do not have a vacuum window conversion, but satisfy the trigger due to accidental drift chamber activity.

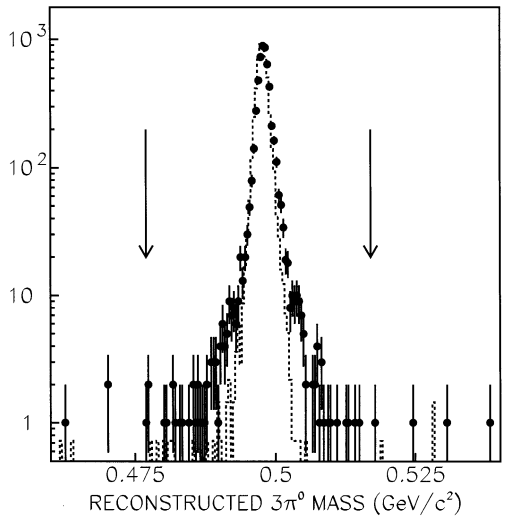

Fig. 4. Reconstructed $3\pi^0$ mass for photon conversion candidates which pass all other cuts. Points with errors are data; dashed histogram is Monte Carlo. The vertical arrows indicate the cut boundaries.

4.3. Charged analysis

Photon conversions are identified using a tracking algorithm with loose timing requirements on hit-pairs in overlapping drift chamber planes. This is necessary to reconstruct conversion pairs with both tracks in the same cell in multiple planes; the signature of two very-close tracks in the chambers is a hit-pair with poor timing. The loose requirement can also be satisfied by accidental out-of-time tracks, so tracks were required to point to a counter in the trigger hodoscopes with an in-time hit (as seen in Fig. 3). Two tracking topologies are accepted as conversion candidates.

4.3.1. One-track events

"One-track" events account for 94.9% of the MC conversion events which pass the calorimeter analysis cuts. These events have a single reconstructed track, which points to one of the six clusters in the CsI. In these events, either the two tracks were too close to be resolved in either the chambers or the calorimeter, or the low-energy track scattered out downstream and produced a cluster below threshold. 5318 events in the charged trigger data sample satisfy this cut.

4.3.2. Two-track events

Only 1.8% of MC conversion events are accepted as "two-track" events. These events have two reconstructed tracks, both of which point to the *same* cluster in the CsI. Because events are required to have only six clusters in the calorimeter analysis, single-conversion events where the two electrons form two different clusters – approximately 3% of all conversions – are rejected earlier, at the calorimeter analysis stage. 304 charged trigger events satisfy the two-track criteria. Adding the one-track events gives a total of 5622 photon conversion candidates.

4.3.3. Conversions which fail the charged analysis

Of MC conversion events which pass the calorimeter analysis, 96.7% also pass either the one-track or two-track charged analysis. On examination of

the 3.3% of MC conversion events which pass the neutral cuts but fail to satisfy either of these two topologies, 80% have two reconstructed tracks; the rest have three from either multiple conversions or accidental tracks.

Of the two-track events, about half have two photons convert (this is consistent with the expected radiation thickness of the vacuum window). The remaining events have two tracks, only one of which is matched to a CsI cluster because the lower-energy track from the conversion was below the threshold for forming a cluster in the CsI. This event loss depends sensitively on how multiple scattering is modeled in the MC, and uncertainty in this inefficiency dominates the systematic error in the vacuuum window measurement (as discussed below).

The various topologies of MC conversions are summarized in Table 1.

4.4. Dalitz background

The largest irreducible background to conversions comes from the π^0 Dalitz decay ($\pi^0 \to e^+e^-\gamma$). Both the final sweeper and the electron separator magnet fields affect the spectrum of Dalitz background; both magnets were simulated using measured field maps.

MC studies showed the expected background from Dalitz decays in the signal region to be 183 ± 11 events (3.4% of conversion candidates) in the one-track case and 37 ± 5 events (12% of candidates) in the two-track case, giving a total of 220 ± 12 events (3.9% of the total conversion candidates). The errors shown for the Dalitz background are from MC statistics. Although this background could be reduced somewhat by cutting events with extra in-time activity in the first chamber, the efficiency of this cut for signal events is difficult to model. Therefore, no further attempt was made to reduce Dalitz background. Fig. 5 shows the Z-distribution of data points along with MC predictions from photon conversions and Dalitz background. As can be seen in the figure, the separator magnet improves the signal-to-background ratio from ~ 1 to about 25.

Table 1
Acceptance categories for six-cluster MC conversion events which pass the calorimeter analysis.

One track, matched to cluster (accepted)	94.9%
Two tracks, matched to same cluster (accepted)	1.8%
Two tracks, matched to different clusters (double conversion topology; rejected)	1.5%
Two tracks, one not matched to any cluster (accidental or low-momentum track scattered; rejected)	1.2%
Three or more tracks (accidental track or multiple conversion; rejected)	0.6%

4.5. Out-of-time track background

Although requiring tracks to match in-time hits in the trigger hodoscopes reduced the out-of-time

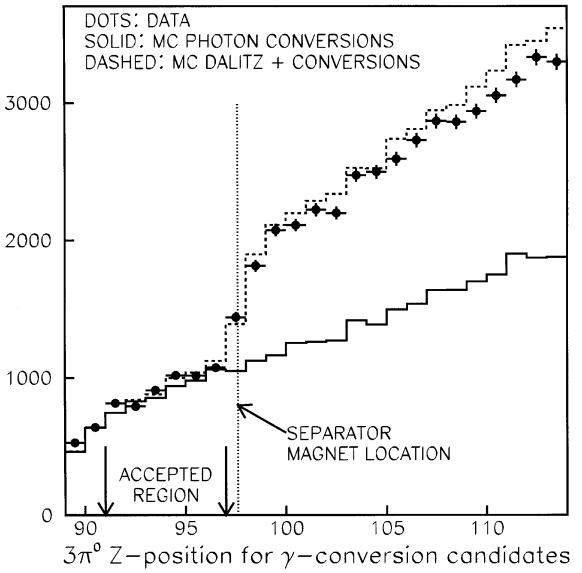

Fig. 5. Z-position (distance from target) of candidate $K_L \to 3\pi^0 \to 6\gamma$ events with a photon conversion. The dots with errors are data; the solid histogram is the MC prediction from conversions alone, normalized to the background-subtracted data points in the accepted region from $Z = 91$ to 97 m. The dashed histogram is the same MC prediction with Dalitz decay background added. The Dalitz background is normalized using the measured rate of $K_L \to 3\pi^0$ decays and the $\pi^0 \to e^+e^-\gamma$ branching ratio. The electron separator magnet at $Z = 97.6$ m greatly suppresses the Dalitz background upstream of it. The Dalitz background downstream of the magnet does not match the MC simulation perfectly, because it is critically sensitive to the modeling of multiple scattering in the detector.

track background greatly, a very small background remained due to accidental in-time hodoscope hits and hits from photons which converted downstream of the first drift chamber. This background is estimated to be 11 ± 11 events (systematic error only).

4.6. Extraction of the photon conversion probability

The background-subtracted conversion signal is 5391 ± 78 events, where the error is statistical only, and includes statistical error on the subtracted backgrounds. Dividing by the MC acceptance gives a total of $(2.29 \pm 0.033) \times 10^5$ $K_L \to 3\pi^0 \to 6\gamma$ decays in the acceptance region where at least one photon converted at the vacuum window.

We divide by the measured number of $K_L \to 3\pi^0$ decays and correct for the $\pi^0 \to \gamma\gamma$ branching ratio, yielding a probability of 0.01645 ± 0.00024 that at least one of six photons converts, or an individual photon conversion probability of $(2.761 \pm 0.040) \times 10^{-3}$ (the error is statistical only).

4.7. Other systematic errors

The radiation length analysis measures the ratio of events with tracks to events without tracks. Tracking efficiency, therefore, enters the calculation at first order. Studies in normal data show the single-track-finding efficiency to be better than 0.99. Although in principle we have two tracks in the event, only one is usually reconstructible. As there is no clean way to measure inefficiency at this level in the radiation length data set, a systematic error of $\pm 1\%$ is assigned.

A larger systematic error comes from modeling of multiple scattering in the detector. This is a dominant source of the acceptance loss for conversions relative to all-neutral decays. The model used in the MC is a parameterization of the Molière theory [6]; all scattering is assumed to occur at the vacuum window, the four chamber planes, and four equally-spaced slices of material which represent the helium bags. Much of the Dalitz background and some of the signal, according to the MC, has at least one track below 0.5 GeV. Typical scattering angles for these tracks in the vacuum window and the chambers are greater than 1 mrad, producing position shifts greater than one cell in the downstream drift chambers. Under these conditions, tracks in the spectrometer may not remain straight enough to be reconstructed, and the approximation that scattering occurs only at the chamber planes becomes invalid. This is seen in the disagreement between the data and MC in the acceptance for Dalitz decay background downstream of the separator magnet (Fig. 5), as well as in the poor prediction of the ratio of two-track to one-track conversion candidates (5% in data after background subtraction, versus 2% in MC).

The effect of multiple scattering on the radiation length measurement was studied by varying all material in the MC scattering simulation upward by a factor of two, and downward to zero. Removing scattering effects caused the reconstructed conversion probability to drop by 0.9% of itself. Doubling the scattering had more effect; it caused the measured conversion probability to increase by 3.7%. We conservatively assign a $\pm 3.7\%$ systematic error to multiple scattering effects.

The pairing χ^2 cut in the calorimeter analysis was an additional source of systematic error. This error was primarily due to miscalibration of the CsI calorimeter, which caused cluster resolutions to be poorer in the data than in the MC. The error was estimated by changing the value of the cut fron 6.25 to 200 (the nominal cut is at 25). The range was chosen to be more than twice the discrepancy between the median χ^2 in the data and MC photon conversion samples. This caused a variation of $\pm 2.7\%$ in the measured conversion probability, and this is taken as the systematic error.

4.8. Calculating the radiation length

At high energies, the probability for a photon to convert in a thin ($\ll X_0$) window is $\frac{7}{9}$ of the thickness of the window in radiation lengths. The error on the measurement of conversion probability is 4.9% of the total (see Table 2), so the conversion probability is $(2.76 \pm 0.13) \times 10^{-3}$. Scaling by $\frac{9}{7}$, the amount of material upstream of the midplane of the first drift chamber is measured to be $(3.55 \pm 0.17) \times 10^{-3} X_0$.

Table 2
Summary of sources of error in radiation length measurement

Conversion statistics	1.5%
Tracking efficiency	1.0%
Trigger hodoscope efficiency	0.2%
Out-of-time track background	0.2%
Pairing χ^2 cut	2.7%
Multiple scattering modeling	3.7%
Total	4.9%

5. Comparison to expected value

The Mylar–Kevlar vacuum window was the largest single component of the material; its radiation thickness was calculated to be $(1.56 \pm 0.16) \times 10^{-3}\ X_0$ [7]. The remaining material was expected to contribute $(1.91 \pm 0.03) \times 10^{-3}\ X_0$, on the assumption that Bag 1a was filled with air and Bag 1b with helium. This yielded a total thickness of $(3.47 \pm 0.16) \times 10^{-3}\ X_0$, which is in very good agreement with the measurement above. It should be noted that this measurement has sufficient sensitivity to probe the composition of the gas volumes; if Bag 1a had been filled with helium instead of air, the radiation thickness would have dropped by $0.78 \times 10^{-3}\ X_0$, which is 4.6 times the sensitivity of this measurement.

6. Conclusion

We have used the technique described here to measure the thickness of a window assembly to an accuracy of $1.7 \times 10^{-4}\ X_0$. With better modeling of multiple scattering of low-energy tracks, the precision could in principle be improved if necessary.

This method measures the integrated material between a magnet and the sense wires of a tracking chamber. It requires a decay mode with photons in the final state, and the decay must be reconstructible with low background without a magnetic field downstream of the material under study. Although we have only used the $K_L \to 3\pi^0$ decay, it might be feasible for other experiments to use $K_S \to \pi^0\pi^0$ or common hyperon or charged kaon decays to one or more π^0's. Backgrounds resulting from decays with internal conversion of a photon (and therefore an e^+e^- pair in the final state) can be removed using a magnet upstream of the material under study.

Acknowledgements

The author wishes to acknowledge R. Ford, D. Jensen, D. Pushka, and J. Volk of Fermi National Accelerator Laboratory for the design and construction of the separator magnet used in this measurement. The E799/E832 collaboration and the author's support from the US Department of Energy and the National Science Foundation are also gratefully acknowledged.

References

[1] T. Nakaya, Ph.D. Thesis, Osaka University, 1995.
[2] R.S. Kessler et al., Nucl. Instr. and Meth A 368 (1996) 653.
[3] EGS4 simulation implemented in local Monte Carlo code.
[4] R. Ford et al., Nucl. Instr. and Meth. A 426 (1999) 238.
[5] C. Bown et al., Nucl. Instr. and Meth. A 369 (1996) 248.
[6] H. Bethe, Phys. Rev. 89 (1953) 1256.
[7] D. Jensen, private communication, 1997.